Synchronized clusters in coupled map networks. I. Numerical studies

Sarika Jalan,[1,*] R. E. Amritkar,[1,†] and Chin-Kun Hu[2,‡]
[1]*Physical Research Laboratory, Navrangpura, Ahmedabad 380 009, India*
[2]*Institute of Physics, Academia Sinica, Nankang, Taipei 11529, Taiwan*
(Received 16 June 2004; published 19 July 2005; corrected 26 July 2005)

We study the synchronization of coupled maps on a variety of networks including regular one- and two-dimensional networks, scale-free networks, small world networks, tree networks, and random networks. For small coupling strengths nodes show turbulent behavior but form phase synchronized clusters as coupling increases. When nodes show synchronized behavior, we observe two interesting phenomena. First, there are some nodes of the floating type that show intermittent behavior between getting attached to some clusters and evolving independently. Second, we identify two different ways of cluster formation, namely self-organized clusters which have mostly intracluster couplings and driven clusters which have mostly intercluster couplings. The synchronized clusters may be of dominant self-organized type, dominant driven type, or mixed type depending on the type of network and the parameters of the dynamics. We define different states of the coupled dynamics by considering the number and type of synchronized clusters. For the local dynamics governed by the logistic map we study the phase diagram in the plane of the coupling constant (ϵ) and the logistic map parameter (μ). For large coupling strengths and nonlinear coupling we find that the scale-free networks and the Caley tree networks lead to better cluster formation than the other types of networks with the same average connectivity. For most of our study we use the number of connections of the order of the number of nodes. As the number of connections increases the number of nodes forming clusters and the size of the clusters in general increase.

DOI: 10.1103/PhysRevE.72.016211 PACS number(s): 05.45.Ra, 05.45.Xt, 89.75.Fb, 89.75.Hc

I. INTRODUCTION

Several complex systems have underlying structures that are described by networks or graphs and the study of such networks is emerging as one of the rapidly growing subjects [1,2]. One significant discovery in the field of complex networks is the observation that a number of naturally occurring large and complex networks come under some universal classes and they can be simulated with simple mathematical models, viz. small-world networks [3], scale-free networks [4], etc. These models are based on simple physical considerations and they give simple algorithms to generate graphs which resemble several actual networks found in many diverse systems such as the nervous systems [5], social groups [6], World Wide Web [7], metabolic networks [8], food webs [9], and citation networks [10].

Several networks in the real world consist of dynamical elements interacting with each other and the interactions define the links of the network. Several of these networks have a large number of degrees of freedom and it is important to understand their dynamical behavior. Here, we study synchronization and cluster formation in networks consisting of interacting dynamical elements.

Synchronization and cluster formation lead to rich spatiotemporal patterns when opposing tendencies, i.e., the nonlinear dynamics of the maps that in the chaotic regime tends to separate the orbits of different elements, and the couplings that tend to synchronize them, compete. There are several studies on coupled maps/oscillators on regular lattices as well as globally coupled networks. Coupled map lattices with nearest neighbor or short range interactions show interesting spatiotemporal patterns and intermittent behavior [11,12]. Globally coupled maps (GCM) where each node is connected with all other nodes, show interesting synchronized behavior [13]. Formation of clusters or coherent behavior and then loss of coherence are described analytically as well as numerically with different viewpoints [14–19]. Chaotic coupled map lattices show beautiful phase ordering of nodes [20]. There are also some studies of coupled maps on different types of networks. References [21–23] shed some light on the collective behavior of coupled maps/oscillators with local and nonlocal connections. Random networks having a large number of connections also show synchronized behavior for large coupling strengths [24–26]. There are some studies on synchronization of coupled maps on Caley tree [27], small-world networks [28–30], and hierarchal organization [31]. Coupled map lattice with sine-circle map gives synchronization plateaus [32]. The analytical stability condition for synchronization of coupled maps for different types of linear and nonlinear couplings are also discussed in several papers [33–36]. Synchronization and partial synchronization of two coupled logistic maps are discussed at length in Ref. [37]. Apart from this there are other studies that explore different properties of coupled maps [38–42].

Coupled maps have been found to be useful in several practical situations. These include fluid dynamics [43], hydrodynamic turbulence [44], nonstatistical behavior in optical systems [45], convection [46,47], stock markets [48], ecological systems [49], logic gates [50], solitons [51],

*Email address: sarika@prl.ernet.in
†Email address: amritkar@prl.ernet.in
‡Email address: huck@phys.sinica.edu.tw

c-elegans [52], cosmology [53], and quantum field theories [54].

Here we study the detailed dynamics of coupled maps on different networks and investigate the mechanism of cluster formation and synchronization properties. We explore the evolution of individual nodes with time and study the role of different connections in forming the clusters of synchronized nodes in such coupled map networks (CMNs).

Most of the earlier studies of synchronized cluster formation have focused on networks with a large number of connections ($\sim N^2$). In this paper, we consider networks with a number of connections of the order of N. This small number of connections allows us to study the role that different connections play in synchronizing different nodes and the mechanism of synchronized cluster formation. The study reveals two interesting phenomena. First, when nodes form synchronized clusters, there can be some nodes which show an intermittent behavior between independent evolution and evolution synchronized with some cluster. Second, the cluster formation can be in two different ways, driven and self-organized phase synchronization [55]. The connections or couplings in the self-organized phase synchronized clusters are mostly of the intracluster type while those in the driven phase synchronized clusters are mostly of the intercluster type. As the number of connections increases more and more nodes are involved in cluster formation and also the coupling strength region where clusters are formed increases in size. For a large number of connections, typically of the order of N^2 and for large coupling strengths, mostly one phase synchronized cluster spanning all the nodes is observed.

Depending on the number and type of clusters we define different states of synchronized behavior. For the local dynamics governed by the logistic map, we study the phase diagram in the $\mu-\epsilon$ plane, i.e., the plane defined by the logistic map parameter and the coupling constant.

The paper is organized as follows. In Sec. II, we give the model for our coupled map networks. We also define phase synchronization and synchronized clusters. Some general properties of synchronized clusters in CMNs are discussed in Sec. III. In Sec. IV, we present our numerical results for synchronization in different networks and illustrate the mechanism of cluster formation. This section includes the study of the phase diagram, Lyapunov exponent plots, behavior of individual nodes, floating nodes, dependence on number of connections, and behavior for different types of networks. Section V considers the circle map. Section VI concludes the paper.

II. COUPLED MAPS AND SYNCHRONIZED CLUSTERS

A. Model of a coupled map network (CMN)

Consider a network of N nodes and N_c connections (or couplings) between the nodes. Let each node of the network be assigned a dynamical variable x^i, $i=1,2,\ldots,N$. The evolution of the dynamical variables is written as

$$x_{t+1}^i = (1-\epsilon) f(x_t^i) + \frac{\epsilon}{k_i} \sum_{j=1}^{N} C_{ij} g(x_t^j), \tag{1}$$

where x_t^i is the dynamical variable of the ith node at time t and ϵ is the coupling constant. The topology of the network is introduced though the adjacency matrix C with elements C_{ij} taking values 1 or 0 depending upon whether i and j are connected or not. C is a symmetric matrix with diagonal elements zero and $k_i=\Sigma C_{ij}$ is the degree of node i. The factors $(1-\epsilon)$ in the first term and k_i in the second term are introduced for normalization. The function $f(x)$ defines the local nonlinear map and the function $g(x)$ defines the nature of coupling between the nodes. Here, we present detailed results for the logistic map,

$$f(x) = \mu x(1-x) \tag{2}$$

governing the local dynamics. We have also considered some other maps for the local dynamics. We have studied different types of linear and nonlinear coupling functions and here discuss the results for the following two types of coupling functions.

$$g(x) = x, \tag{3a}$$

$$g(x) = f(x). \tag{3b}$$

We refer to the first type of coupling function as linear and the later as nonlinear. Note that the nonlinear coupling function [Eq. (3b)] is equivalent to a diffusive type of coupling with the diffusion being equally likely along all the connections from any given node.

B. Phase synchronization and synchronized clusters

Synchronization of coupled dynamical systems [56–58] is manifested by the appearance of some relation between the functionals of different dynamical variables. The exact synchronization corresponds to the situation where the dynamical variables for different nodes have identical values. The phase synchronization corresponds to the situation where the dynamical variables for different nodes have some definite relation between their phases [59–62]. When the number of connections in the network is small ($N_C \sim N$) and when the local dynamics of the nodes [i.e., function $f(x)$] is in the chaotic zone, and we look at exact synchronization, we find that only a few synchronized clusters with a small number of nodes are formed. However, when we look at phase synchronization, synchronized clusters with a larger number of nodes are obtained. Hence in our numerical study we concentrate on phase synchronization. We define phase synchronization as follows [63].

Let ν_i and ν_j denote the number of times the dynamical variables x_t^i and x_t^j, $t=t_0,t_0+1,2,\ldots,t_0+T-1$, for the nodes i and j show local minima during the time interval T starting from some time t_0. Here the local minimum of x_t^i at time t is defined by the conditions $x_t^i < x_{t-1}^i$ and $x_t^i < x_{t+1}^i$. Let ν_{ij} denote the number of times these local minima match with each other, i.e., occur at the same time. We define the phase distance, d_{ij}, between the nodes i and j by the following relation [64]:

$$d_{ij} = 1 - \frac{\nu_{ij}}{\max(\nu_i, \nu_j)}. \tag{4}$$

Clearly, $d_{ij}=d_{ji}$. Also, $d_{ij}=0$ when all the minima of variables x^i and x^j match with each other and $d_{ij}=1$ when none of the

minima match. In the Appendix, we show that the above definition of phase distance satisfies metric properties. We say that the nodes i and j are phase synchronized if $d_{ij}=0$, and we define a phase synchronized cluster as a cluster of nodes in which all the pairs of nodes are phase synchronized. In the subsequent discussion the word "phase" is omitted when the meaning is clear.

III. GENERAL PROPERTIES OF SYNCHRONIZED DYNAMICS

We consider some general properties of synchronized dynamics. They are valid for any coupled discrete and continuous dynamical systems. Also, these properties are applicable for exact as well as phase synchronization and are independent of the type of network.

A. Behavior of individual nodes

As the network evolves, it splits into several synchronized clusters. Depending on their asymptotic dynamical behavior the nodes of the network can be divided into three types.

(a) *Cluster nodes:* A node of this type synchronizes with other nodes and forms a synchronized cluster. Once this node enters a synchronized cluster it remains in that cluster afterwards.

(b) *Isolated nodes:* A node of this type does not synchronize with any other node and remains isolated all the time.

(c) *Floating nodes:* A node of this type keeps on switching intermittently between an independent evolution and a synchronized evolution attached to some cluster.

Of particular interest are the floating nodes and we will discuss some of their properties afterwards.

B. Mechanism of cluster formation

The study of the relation between the synchronized clusters and the couplings between the nodes represented by the adjacency matrix C shows two different mechanisms of cluster formation [55].

(i) Self-organized clusters: The nodes of a cluster can be synchronized because of intracluster couplings [see, e.g., Fig. 3(b)]. We refer to this as the self-organized synchronization and the corresponding synchronized clusters as self-organized clusters.

(ii) Driven clusters: The nodes of a cluster can be synchronized because of intercluster couplings [see, e.g., Fig. 3(d)]. Here the nodes of one cluster are driven by those of the others. We refer to this as the driven synchronization and the corresponding clusters as driven clusters.

In our numerical studies we have been able to identify ideal clusters of both types, as well as clusters of the mixed type where both ways of synchronization contribute to cluster formation. We will discuss several examples to illustrate both types of clusters.

Geometrically the two mechanisms of cluster formation can be easily understood by considering a tree type network. A tree can be broken into different clusters in different ways.

(a) A tree can be broken into two or more disjoint clusters with only intracluster couplings by breaking one or more connections. Clearly, this splitting is not unique and will lead to self-organized clusters.

(b) A tree can also be divided into two clusters by putting connected nodes into different clusters. This division is unique and leads to two clusters with only intercluster couplings, i.e., driven clusters.

(c) Several other ways of splitting a tree are possible. For example, it is easy to see that a tree can be broken into three clusters of the driven type.

Quantitative measure for self-organized and driven behavior. To get a clear picture of self-organized and driven behavior we define two quantities f_{intra} and f_{inter} as measures for the intracluster and intercluster couplings as follows:

$$f_{\text{intra}} = \frac{N_{\text{intra}}}{N_c}, \tag{5a}$$

$$f_{\text{inter}} = \frac{N_{\text{inter}}}{N_c}, \tag{5b}$$

where N_{intra} and N_{inter} are the numbers of intra- and intercluster couplings, respectively. In N_{inter}, couplings between two isolated nodes are not included. The quantities f_{intra} and f_{inter} allow us to determine the dominant behavior when there are several clusters and it is not easy to identify the main mechanism of cluster formation.

C. States of synchronized dynamics

Normally, the states of coupled dynamical systems are classified on the basis of the number of clusters as in Ref. [65]. Our finding of two mechanisms of cluster formation allow us to refine this classification.

(a) Turbulent state (I-T): All nodes behave chaotically with no cluster formation.

(b) Partially ordered state (III): Nodes form a few clusters with some isolated nodes not attached to any cluster. We can further subdivide the clusters of the partially ordered state into subcategories depending on the type of clusters, i.e., self-organized (S), driven (D), or mixed type (M).

(c) Ordered state (IV): Nodes form two or more clusters with no isolated nodes. The ordered state can be further divided into three substates based on the nature of dynamics of the synchronized clusters as chaotic ordered state (C), quasiperiodic ordered state (Q), and periodic ordered state (P). Also, as for the partially ordered state we can have subcategories as self-organized (S), driven (D), or mixed type (M).

(d) Coherent state (V): Nodes form a single synchronized cluster. The dynamical behavior is usually periodic (P) or of a fixed point (F).

(e) Variable state (II): Nodes form different states, partially ordered or ordered state depending on the initial conditions.

IV. NUMERICAL RESULTS

Now we present the numerical results for the CMNs on different types of networks. The adjacency matrix C depends on the type of network and $C_{ij}=1$ if the corresponding nodes in the network are connected and zero otherwise. Starting

from random initial conditions the dynamics of Eq. (1), after an initial transient, leads to interesting phase synchronized behavior.

A. Coupled maps on scale-free network

First we present a detailed discussion of our numerical results for the scale-free network. Other types of networks will be discussed briefly indicating the similarities and differences in the behavior.

1. Generation of network

The scale-free network of N nodes is generated by using the model of Barabasi *et al.* [66]. Starting with a small number, m_0, of nodes, a new node with $m \leqslant m_0$ connections is added at each time step. The probability $\pi(k_i)$ that a connection starting from this new node is connected to a node i depends on the degree k_i of node i (preferential attachment) and is given by

$$\pi(k_i) = \frac{(k_i + 1)}{\sum_j (k_j + 1)}.$$

After τ time steps the model leads to a network with $N = \tau + m_0$ nodes and $m\tau$ connections. This model leads to a scale-free network, i.e., the probability $P(k)$ that a node has degree k decays as a power law,

$$P(k) \sim k^{-\lambda},$$

where λ is a constant and for the type of probability law $\pi(k)$ that we have used $\lambda = 3$. Other forms for the probability $\pi(k)$ are possible which give different values of λ. We have tried out a few more forms of $\pi(k)$ giving different values of λ and we find results similar to the ones reported here. This indicates that the exact form of $\pi(k)$ is probably not important for the properties that we have studied.

2. Linear coupling

Phase diagram. First we consider the linear coupling, $g(x) = x$. Figure 1 shows the phase diagram in the two parameter space defined by μ and ϵ for the scale-free network with $m = m_0 = 1$, $N = 50$, and $T = 100$. For $m = 1$, the network has a tree structure. The behavior for larger m values will be discussed afterwards. The different regions of the phase diagram are labeled as explained in the Sec. III C. For $\mu < 3$, we get a stable coherent region (region V-F) with all nodes having the fixed point value. To understand the remaining phase diagram, consider the line $\mu = 4$. Figure 2 shows the largest Lyapunov exponent λ as a function of the coupling strength ϵ for $\mu = 4$. For small values of ϵ, we observe turbulent behavior with all nodes evolving chaotically and there is no phase synchronization (region I-T). Figure 3 shows node-node plots of the synchronized clusters with any two nodes belonging to the same cluster shown as open circles and the couplings between the nodes ($C_{ij} = 1$) shown as closed circles. Turbulent behavior with no synchronization is shown in Fig. 3(a). There is a critical value of the coupling strength ϵ_c beyond which synchronized clusters can be observed. This

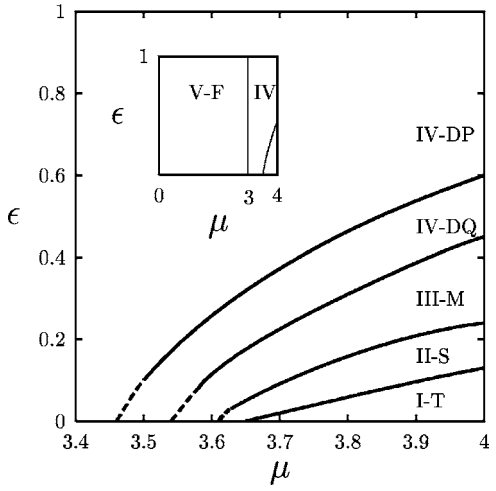

FIG. 1. Phase diagram showing different regions in the two parameter space of μ and ϵ for the scale-free network for $f(x) = \mu x(1-x)$ and $g(x) = x$. Different regions are I: turbulent region, II: region with varying behavior, III: partially ordered region, IV: ordered region, and V: coherent region. The symbols T, S, M, D, P, Q, and F, respectively, correspond to turbulent behavior, self-organized synchronization, mixed synchronization, driven synchronization, periodic, quasiperiodic, and fixed point behavior. Region boundaries are determined based on the asymptotic behavior using several initial conditions, number of clusters and isolated nodes, synchronization behavior, and also the behavior of the largest Lyapunov exponent. The dashed lines indicate uncertainties in determining the boundaries. Calculations are for $N = 50$, $m = 1$, and $T = 100$. The inset shows the phase diagram for the entire range of parameter μ, i.e., from 0 to 4.

is a general property of all CMNs and the exact value of ϵ_c depends on the type of network, the type of coupling function, and the parameter μ.

As ϵ increases beyond ϵ_c, we get into a variable region (region II-S) which shows a variety of phase synchronized behavior, namely ordered chaotic, ordered quasiperiodic, ordered periodic, and partially ordered behavior depending on

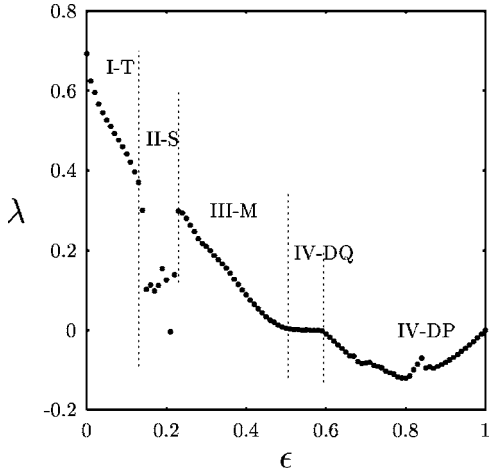

FIG. 2. Largest Lyapunov exponent, λ, is plotted as a function of ϵ for the scale-free network and $f(x) = 4x(1-x)$ and $g(x) = x$. Different regions are labeled as in Fig. 1.

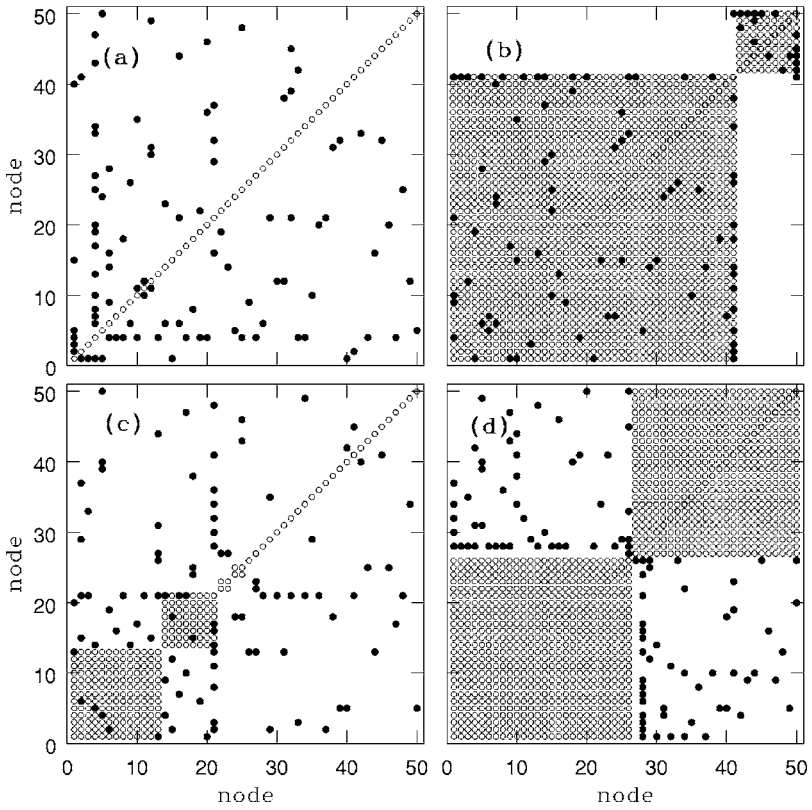

FIG. 3. The figure shows node vs node diagrams for several examples illustrating the self-organized and driven phase synchronization and the variety of clusters that are formed. After an initial transient (about 2000 iterates) phase synchronized clusters are studied for $T=100$. The examples are for a scale-free network with $N=N_c+1=50$ and the logistic map parameter $\mu=4$ and the coupling function $g(x)=x$. The closed circles show that the two corresponding nodes are coupled (i.e., $C_{ij}=1$) and the open circles show that the corresponding nodes are phase synchronized. In each case the node numbers are reorganized so that nodes belonging to the same cluster are numbered consecutively and the clusters get displayed in decreasing sizes. (a) Turbulent phase for $\epsilon=0.10$. (b) An ideal self-organized phase synchronization for $\epsilon=0.16$. (c) Mixed behavior for $\epsilon=0.32$. (d) An ideal driven phase synchronization for $\epsilon=0.90$. The scale-free networks were generated with $N_0=1$ and $m=1$.

the initial conditions. The mechanism of cluster formation is of dominant self-organized type. In the middle of region II-S, we can observe ideal self-organized behavior with two clusters [Fig. 3(b)] [67].

The next region (region III-M) shows partially ordered chaotic behavior. Here, the number of clusters as well as the number of nodes in the clusters depend on the initial conditions and also they change with time. There are several isolated nodes not belonging to any cluster and floating nodes which keep on switching intermittently between an independent evolution and a phase synchronized evolution attached to some cluster. The synchronized clusters are of the mixed type where both mechanisms of cluster formation contribute and intracluster and intercluster connections are almost equal in number [Fig. 3(c)].

The last two regions (IV-DQ and IV-DP) are ordered quasiperiodic and ordered periodic regions showing driven synchronization. In these regions, the network always splits into two clusters. The two clusters are perfectly antiphase synchronized with each other, i.e., when the nodes belonging to one cluster show minima those belonging to the other cluster show maxima. Figure 3(d) shows the node-node plot of ideal driven synchronization obtained in the middle of region IV-DP [67]. The phenomena of driven synchronization in this region is a very robust one in the sense that it is obtained for almost all initial conditions, the transient time is very small, the nodes belonging to the two clusters are uniquely determined, and we get a stable solution.

We note that region III-M acts as a crossover region from the self-organized to the driven behavior. Here, the clusters are of the mixed type and there is a competition between the self-organized and driven behavior. This appears to be the reason for the formation of several clusters and floating nodes as well as the sensitivity of these to the initial conditions.

Figure 4 shows the plot of f_{intra} and f_{inter} [Eq. (5b)] as a function of the coupling strength ϵ. The figure gives a clear picture of the different features of the phase diagram discussed above. It shows that for small coupling strength (turbulent region I-T) both f_{intra} and f_{inter} are zero indicating that there is no cluster formation. In region II-S, we get f_{intra}

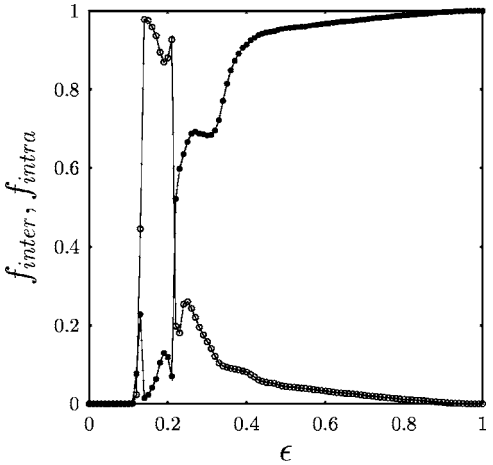

FIG. 4. The fraction of intracluster and intercluster couplings, f_{inter} (closed circles) and f_{intra} (open circle), is shown as a function of the coupling strength ϵ for the scale-free networks with $f(x)=4x(1-x)$ and $g(x)=x$. (The lines connect the points and are drawn as a guide to the eye.) The figure is obtained by averaging over 20 realizations of the network and 50 random initial conditions for each realization.

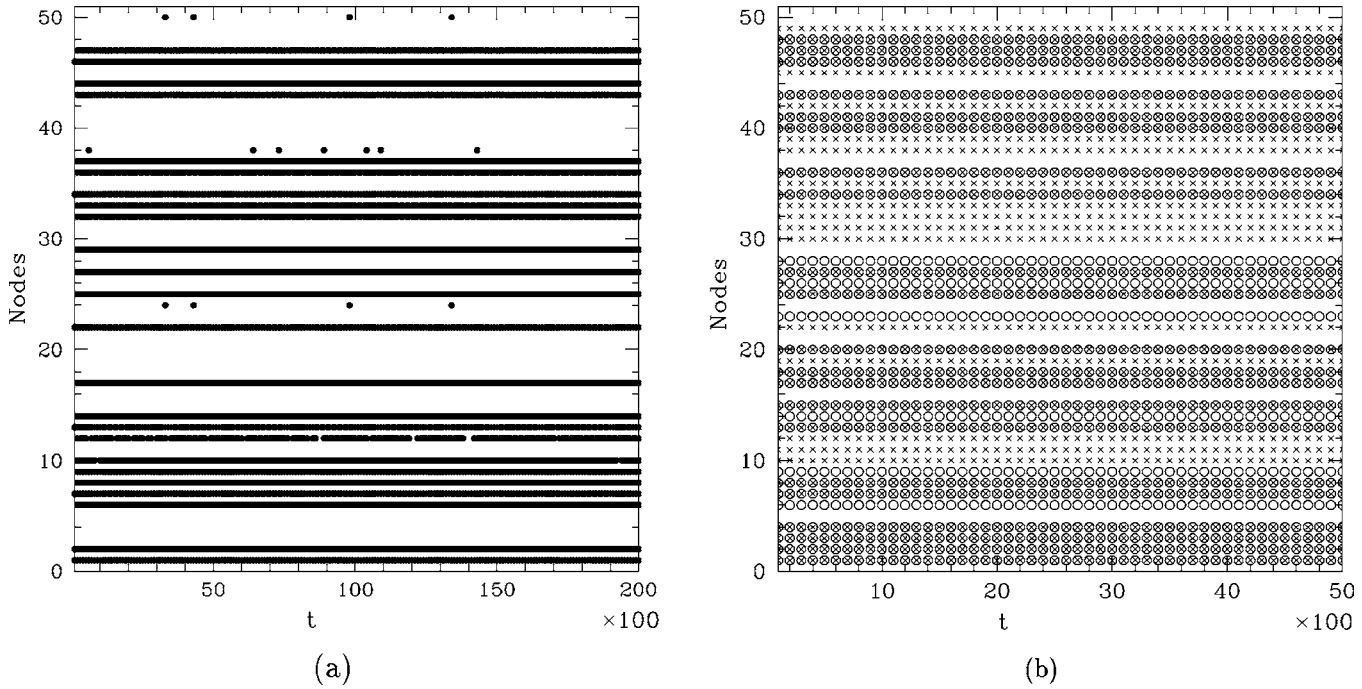

FIG. 5. (a) The time evolution of nodes in a cluster for a scale-free network with both cluster nodes and floating nodes. The nodes belonging to the cluster are shown by closed circles. Here, $\epsilon=0.4$, $f(x)=\mu x(1-x)$, and $g(x)=x$. Node numbers 12, 24, 38, and 50 are of the floating type. They spend some time intermittently in a synchronized evolution with the given cluster and the remaining time in either a synchronized evolution with other clusters or in an independent evolution as an isolated node. (b) Figure shows two stationary clusters of self-organized type for $\epsilon=0.19$ and $g(x)=x$. The two clusters are for the same ϵ value but obtained from two different initial conditions and are denoted by open circles and crosses. Note that some nodes are common to both the clusters while some are different. This illustrates the nonuniqueness of nodes belonging to self-organized clusters depending on the initial conditions.

~ 1 at $\epsilon \sim 0.2$ showing that there are only intracluster couplings leading to self-organized clusters. As coupling strength increases further f_{intra} decreases and f_{inter} increases, i.e., there is a crossover from self-organized to driven behavior (regions III-M). Finally, in regions IV-DQ and IV-DP, we find that f_{inter} is large which shows that in this region most of the connections are of the intercluster type. In region IV-DP we get f_{inter} almost one corresponding to an ideal driven synchronized behavior.

Behavior of individual nodes forming clusters. Now we explore the time evolution of individual nodes. Figure 5(a) shows nodes belonging to one of the synchronized clusters as a function of time for $\epsilon=0.4$ (region III-M) where the symbols (closed circles) indicate the time for which a given node belongs to that cluster. We observe that there are some nodes which intermittently leave the cluster, evolve independently, or get attached with some other cluster and after some time again come back to the same cluster, e.g., the nodes 12 and 24 in Fig. 5(a). These are the floating nodes discussed in Sec. III A. Note that the node 12 spends about 90% of its time in phase synchronization with the given cluster while for the node 24 this time is about 10%.

Let τ denote the residence time of a floating node in a cluster (i.e., the continuous time interval that the node is in a cluster). Figure 6 plots the frequency of residence time $\nu(\tau)$ of a floating node as a function of the residence time τ. A good straight line fit on a log-linear plot shows an exponential dependence,

$$\nu(\tau) \sim \exp(-\tau/\tau_r), \tag{6}$$

where τ_r is the typical residence time for a given node. We have also studied the distribution of the time intervals for which a floating node is not synchronized with a given cluster. This also shows an exponential distribution.

Figure 5(b) demonstrates the nonuniqueness of the self-organized clusters. The figure shows a set of nodes (crosses)

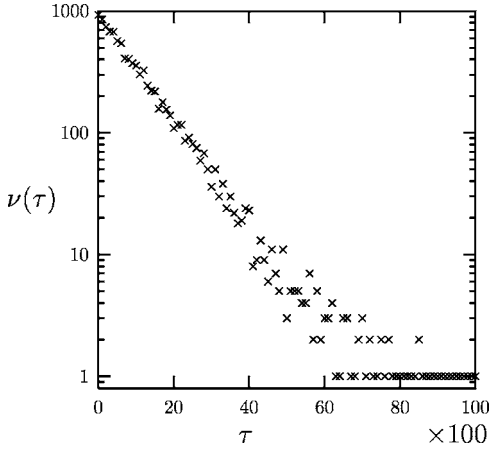

FIG. 6. The figure plots the frequency of residence time $\nu(\tau)$ of a floating node in a cluster as a function of the residence time τ. The data is for the node No. 12 in Fig. 5(a). A good straight line fit on log-linear plot shows exponential dependence.

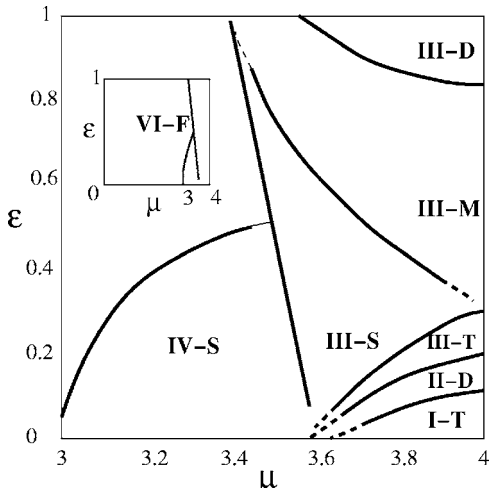

FIG. 7. Phase diagram in the two parameter space of μ and ϵ for the scale-free network for $f(x)=\mu x(1-x)$ and $g(x)=f(x)$. The determination of region boundaries and their classification and symbols are as explained in Fig. 1. Calculations are for $N=50$, $m=1$, and $T=100$. The inset shows the phase diagram for the entire range of parameter μ, i.e., from 0 to 4.

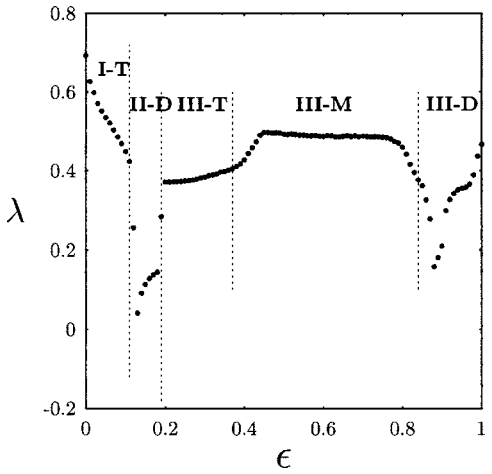

FIG. 8. Largest Lyapunov exponent, λ, is plotted as a function of ϵ for a scale-free network with $f(x)=4x(1-x)$ and $g(x)=f(x)$. Different regions are labeled as in Fig. 7.

belonging to a cluster for $\epsilon=0.19$ (region II-S) and another set of nodes (open circles) belonging to another cluster for the same ϵ but obtained with different initial conditions. For this ϵ value the nodes form self-organized clusters with no isolated nodes. Comparing the members of the two clusters which are obtained from different initial conditions we see that there are some common nodes while some are different. This demonstrates that the splitting of nodes into self-organized clusters is not unique (see Sec. III B). On the other hand, driven synchronization (region IV-DP) mostly leads to a unique cluster formation and does not depend on the initial conditions.

3. Nonlinear coupling

Now we discuss the results for the nonlinear coupling of the type $g(x)=f(x)$. As noted earlier this is equivalent to a diffusive type of coupling. The phase space diagram in the $\mu-\epsilon$ plane is plotted in Fig. 7. Here we do not get clear and distinct regions as we get for the $g(x)=x$ form of coupling. For $\mu<3.5$, we get coherent behavior (regions V-P and VI-F). To describe the remaining phase diagram consider the $\mu=4$ line. Figures 8 and 9 show, respectively, the largest Lyapunov exponent and f_{intra} and f_{inter} as a function of the coupling strength ϵ for $\mu=4$. For small coupling strengths no cluster is formed and we get the turbulent region (I-T). As the coupling strength increases we get into the variable region (II-D). In this region we get a partially ordered and ordered chaotic phase depending on the initial conditions and the clusters of dominant driven type. In a small portion in the middle of region II-D, all nodes form two ideal driven clusters. These two clusters are perfectly antiphase synchronized with each other. Interestingly the dynamics still remains chaotic. Figure 10(a)(a) shows the node-node plot as in Fig. 3 demonstrating ideal driven clusters in the middle of region II-D.

In region III-T, we get almost turbulent behavior with very few nodes forming synchronized clusters. Regions III-M and III-D are partially ordered chaotic regions. In these regions some nodes form clusters and several nodes are isolated or of the floating type. In region III-M, the clusters are of the mixed type (both inter- and intra-cluster couplings) while in region III-D the clusters are of the dominant driven type (see Fig. 9). In these regions, we get phase synchronized clusters but both the size of clusters as well as the number of nodes forming clusters are small. Figures 10(b) and 10(c) are node-node plots demonstrating typical cluster formation in regions III-M and III-D, respectively.

It is interesting to note that for the scale-free network and for the nonlinear coupling, the largest Lyapunov exponent is always positive (Fig. 8), i.e., the whole system remains chaotic but we get phase-synchronized behavior.

We have found significant differences in the synchronization properties for the linearly and nonlinearly coupled maps.

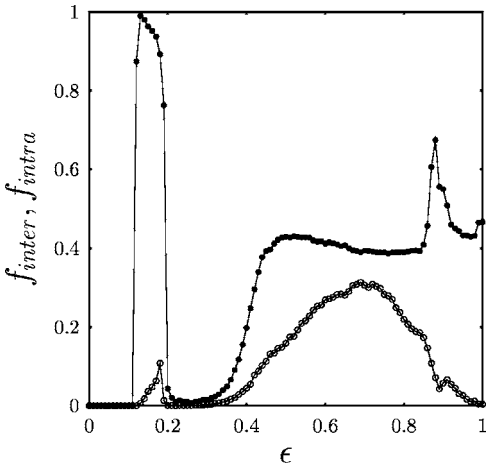

FIG. 9. The fraction of intracluster and intercluster couplings, f_{inter} (closed circles) and f_{intra} (open circles), is shown as a function of the coupling strength ϵ for the scale-free networks with $g(x)=f(x)$. The figure is obtained by averaging over 20 realizations of the network and 50 random initial conditions for each realization.

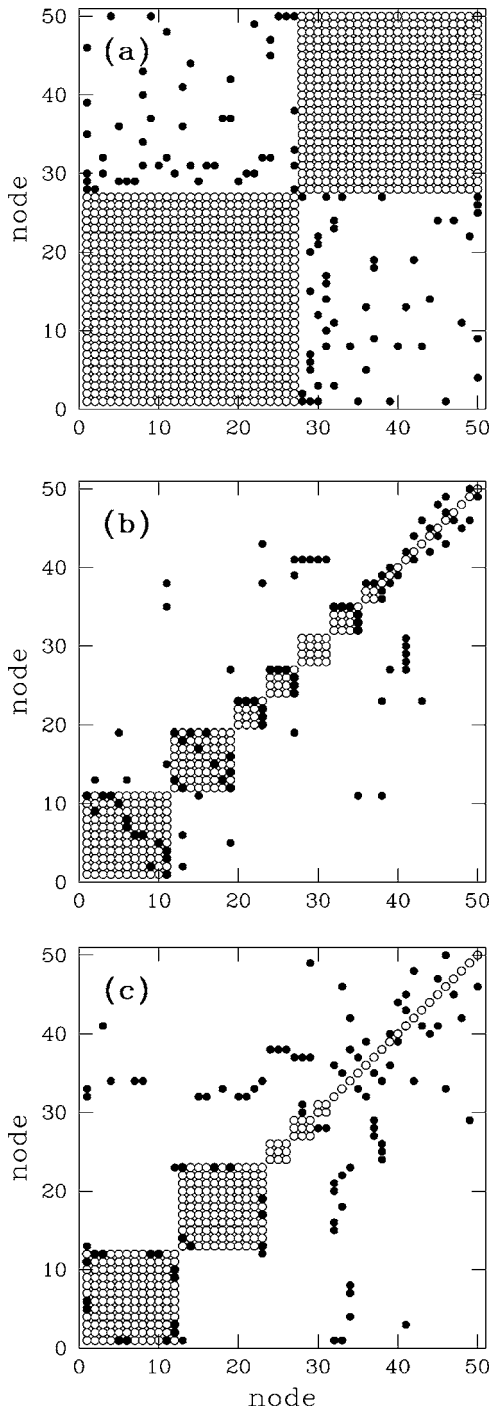

FIG. 10. Examples illustrating the phase synchronization for a scale-free network with coupling form $g(x)=f(x)$ using node vs node diagram for a scale-free network as in Fig. 3. (a) An ideal driven phase synchronization for $\epsilon=0.13$. (b) Mixed behavior for $\epsilon=0.71$. (c) A dominant driven behavior for $\epsilon=0.88$.

Differences in the behavior of linearly and nonlinearly coupled maps have been noted before in connection with other properties [68].

4. Dependence on the number of connections

So far we have treated the scale-free network with $m=1$ which gives a tree structure and the number of connections is of the order of the number of nodes ($N_c=N-1$). As m increases the number of connections increases.

For $m>1$ and $g(x)=x$ the dynamics of Eq. (1) leads to a similar phase diagram as in Fig. 1 with region II-S dominated by self-organized synchronization and regions IV-DQ and IV-DP dominated by driven synchronization. Though perfect inter- and intra-cluster couplings between the nodes as displayed in Figs. 3(b) and 3(d) are no longer observed, clustering in the region II-S is such that most of the couplings are of the intracluster type while for the regions IV-DQ and IV-DP they are of the intercluster type. As m increases the regions I and II are mostly unaffected, but the region IV shrinks and the region III grows in size. Figure 11(a) is a node-node plot for $m=3$ in region II-S ($\epsilon=0.19$) showing two clusters. It is clear that synchronization of nodes is mainly because of intracluster connections but there are a few intercluster connections also. Figure 11(b) is a node-node plot for the ordered periodic region at coupling strength $\epsilon=0.78$. Here the clusters are mainly of the driven type but they have intracluster connections also. Note that for Figs. 11(a) and 11(b) the average degree of a node is 6, and breaking the network into clusters with only intercluster or intracluster couplings is not possible. As the average degree of a node increases further and the number of connections become of the order of N^2, self-organized behavior starts dominating and for large values of ϵ we get one big synchronized cluster.

For $m>1$ and $g(x)=f(x)$ we get a similar kind of behavior as for $m=1$ (Fig. 7) with dominant driven clusters for most of the coupling strength region, but we do not get any ideal driven clusters. Figure 11(c) is a node-node plot for coupling strength $\epsilon=0.9$ and $m=3$. As m increases the region I showing turbulent behavior remains unaffected, but the region II grows in size while the region III shrinks. As m increases more and more nodes participate in cluster formation. The driven behavior decreases in strength with increasing m and self-organized behavior increases in strength. For $m=10$, all nodes form one cluster for larger ϵ values which is obviously of the self-organized type [Fig. 11(d)].

We have also studied the effect of size of the network on the synchronized cluster formation. The phenomena of self-organized and driven behavior persists for the largest size network that we have studied ($N=1000$). The region II showing self-organized or driven behavior is mostly unaffected while the ordered regions showing driven behavior for large coupling strengths show a small shrinking in size.

B. Coupled maps on different networks

We now consider several other networks and investigate synchronization properties of these networks.

1. One-dimensional networks

For one-dimensional CMN, each node is connected with m nearest neighbors (degree per node is $2m$). First we consider $m=1$, i.e., each map is connected with just next neighbors on both sides and we take the open boundary condition. Note that this a tree structure with $N_c=N-1$. Figures 12(a) and 12(b) show f_{intra} and f_{inter} versus ϵ for $\mu=4$, $N=50$, and,

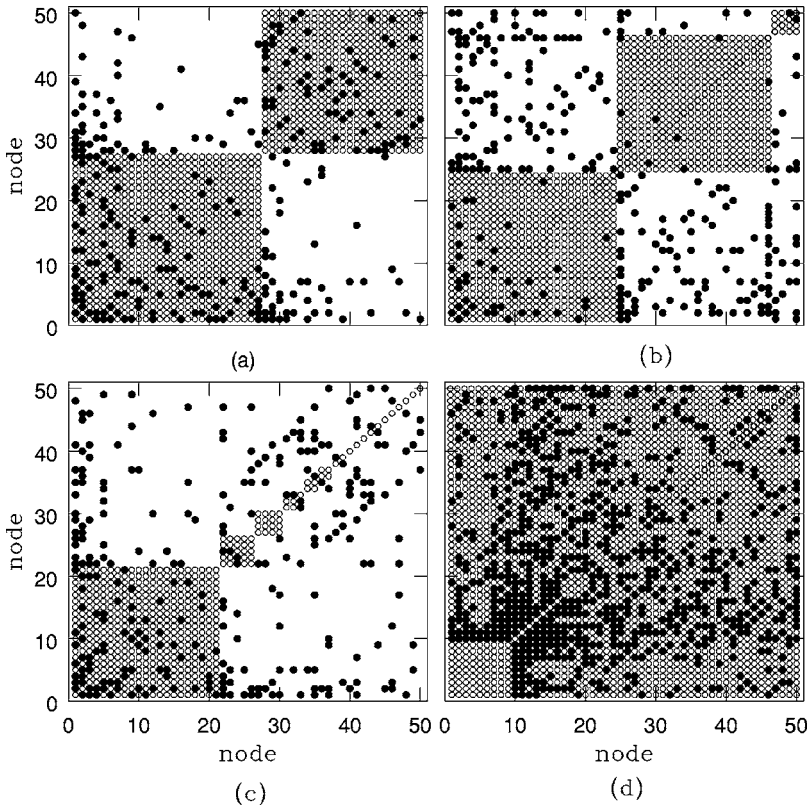

FIG. 11. The cluster formation for the scale-free network as node vs node plot for $N=50$ as in Fig. 3 but with a larger number of connections. (a) and (b) are plotted for $g(x)=x$ and $m=3$ and, respectively, for $\epsilon=0.19$ and $\epsilon=0.78$. (c) and (d) are plotted for $g(x)=f(x)$, $\epsilon=0.90$ and, respectively, for $m=3$ and $m=10$.

respectively, for $g(x)=x$ and $g(x)=f(x)$. For $g(x)=x$, the behavior of clusters as well as the phase diagram and Lyapunov exponent graph are very similar to the scale-free network with the coupling form $f(x)=x$.

However, for $g(x)=f(x)$ coupling and $m=1$ we observe a considerable deviation from the corresponding behavior for the scale-free network. In region I-T of Fig. 7, we get turbulent behavior as for the scale-free network. But we observe clusters only in the region corresponding to the region II-D in Fig. 7. These clusters are of the driven type [Fig. 12(b)]. For the rest of the coupling strength region, i.e., region III in Fig. 7, there is almost no cluster formation and the behavior is close to turbulent and chaotic.

Figure 13(a) shows a node-node plot of two clusters of the mixed type and several isolated nodes for ϵ in region III-M for $g(x)=x$. Figure 13(b) shows a node-node plot of driven clusters for an ϵ value in the region II-D for $g(x)=f(x)$.

We now consider the case $m>1$. For $g(x)=x$ as m increases, i.e., the number of connections increases, the behavior is similar to that of the scale-free network.

For $g(x)=f(x)$ and $m>1$, we find that as the number of connections increases we get two dominant driven phase synchronized clusters as for $m=1$ in region II-D. For large coupling strength the number of nodes forming clusters and the sizes of clusters both increase with the increase in the number of connections. This behavior is seen in Figs. 12(c) and 12(d) which show f_{intra} and f_{inter} versus ϵ for $g(x)=f(x)$, $\mu=4$, and, respectively, for $m=5$ and $m=10$. Figure 14(a) shows the fraction of nodes forming clusters as a function of the number of connections N_c normalized with respect to the maximum number of connections $N_m=N(N-1)/2$ for two values of ϵ. The overall increase in the number of nodes forming clusters is clearly seen. Figure 14(b) shows the fraction of nodes in the largest cluster as a function N_c for two values of ϵ. The overall growth in the size of the clusters with N_c is evident.

Cluster formation with a large number of connections (of the order of N^2) and its dependence on the coupling strength is discussed in Refs. [69,70]. It is reported that for these networks it is the coupling strength which affects the synchronized clusters and not the number of connections. However, as discussed above, we find that when the number of connections is of the order of N the size of the clusters and the number of nodes forming clusters increase as the number of connections increases. This behavior approaches the reported behavior [69,70] as the number of connections becomes of the order of N^2.

2. Small world networks

Small world networks are constructed using the following algorithm by Watts and Strogatz [3]. Starting with a one-dimension ring lattice of N nodes in which every node is connected to its nearest k neighbors ($k/2=m$), we randomly rewire each connection of the lattice with probability p such that self-loops and multiple connections are excluded. Thus $p=0$ gives a regular network and $p=1$ gives a random network. The typical small world behavior is observed around $p=0.01$. We find that for $g(x)=x$, the synchronization behavior is very similar to that for the scale-free networks and one-dimensional lattice. We note that this result for $g(x)=x$ is a general result and appears to be valid for all the networks with the same number of connections. But, for $g(x)=f(x)$, nodes form clusters only for region II-D of coupling strength and there is almost no cluster formation for larger values of

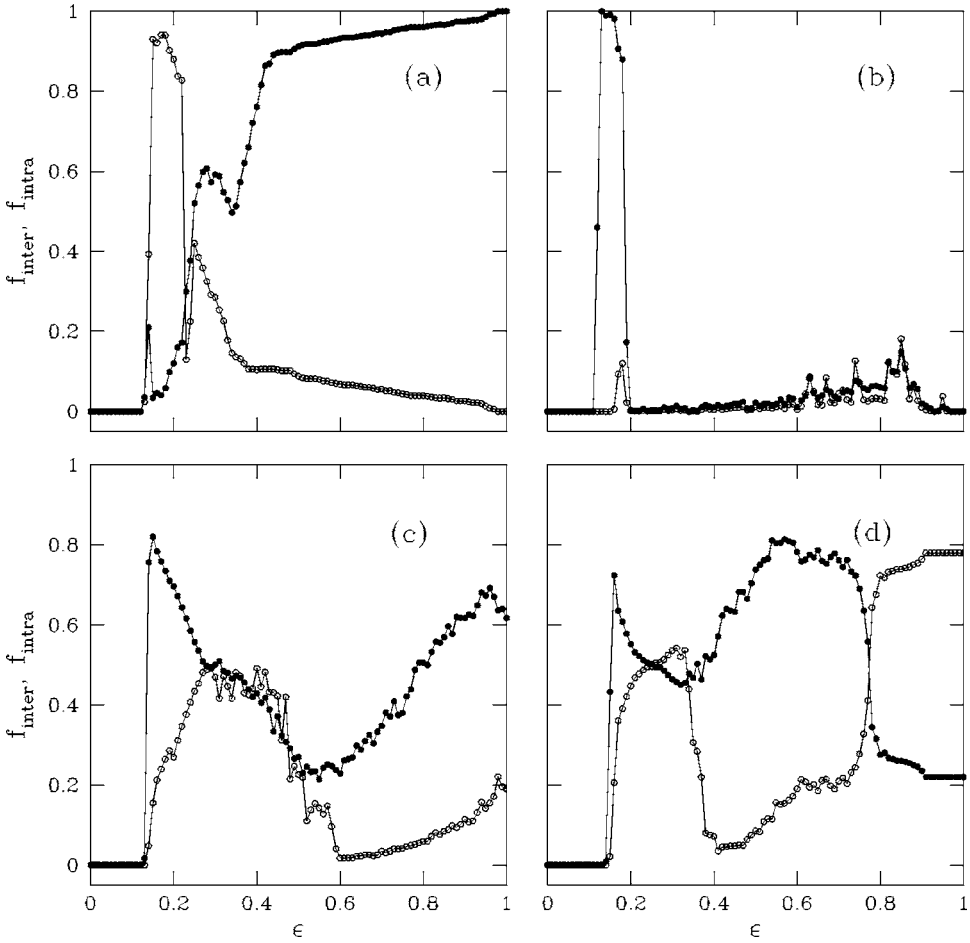

FIG. 12. The fraction of intracluster and intercluster couplings, f_{inter} (closed circles) and f_{intra} (open circles), are shown as a function of the coupling strength ϵ. (a) and (b) are for the one-dimensional coupled maps with nearest neighbor coupling ($m=1$) and for $g(x)=x$ and $g(x)=f(x)$, respectively. (c) and (d) are for $g(x)=f(x)$ and, respectively, $m=5$ and $m=10$.

ϵ. This trend can be seen from Fig. 15(a) where we plot f_{intra} and f_{inter} for $g(x)=f(x)$ as a function of ϵ for $p=0.06$, $\mu=4$, $N=50$, and $k=2$. As k increases, we observe some clusters for large ϵ values. This behavior is similar to that of the one-dimensional network.

3. Caley tree

We generate a Caley tree using the algorithm given in Ref. [27]. Starting with three branches at the first level, we split each branch into two at subsequent levels. For $g(x)=x$, the synchronization behavior is similar to all other networks with the same number of connections. For $g(x)=f(x)$ all nodes form driven clusters for region II-D, and for larger coupling strengths about 40% of nodes form clusters of the dominant driven type [Fig. 15(b)].

4. Higher dimensional lattices

First we consider the two-dimensional square lattice with nearest neighbor interactions. Figures 15(c) and 15(d) plot f_{intra} and f_{inter} for $g(x)=x$ and $g(x)=f(x)$, respectively, as a function of ϵ for $\mu=4$. For $g(x)=x$ the cluster formation is similar to other networks described earlier except for very large ϵ close to one where we get a single self-organized cluster. For $g(x)=f(x)$ cluster formation is similar to that in one-dimensional networks with nearest and next nearest neighbor couplings. In small coupling strength region II-D (see Fig. 7), nodes form two clusters of the driven type and for large coupling strength driven clusters are observed with about 25–30% nodes showing synchronized behavior [Fig. 15(d)].

Coupled maps on three-dimensional cubic lattice (degree per node is six) for $g(x)=x$ show clusters similar to the other networks discussed earlier. For $g(x)=f(x)$, nodes form driven clusters in region II-D and mostly we observe three clusters. For large coupling strengths nodes form driven clusters and the nodes participating in cluster formation are now much larger than the two-dimensional case.

5. Random networks

Random networks are constructed by connecting each pair of nodes with probability p. First consider the case where the average degree per node is two. For linear coupling $g(x)=x$ cluster formation is the same as for other networks with the same average degree. For $g(x)=f(x)$ driven clusters are observed in region II-D and no significant cluster formation is observed for larger coupling strengths. This behavior is similar to the one-dimensional network with $k=2$ but different from the corresponding behavior for the scale-free network. For coupled maps on random networks with the average degree per node equal to four and $g(x)=f(x)$, clusters with dominant driven behavior are observed for all $\epsilon > \epsilon_c$.

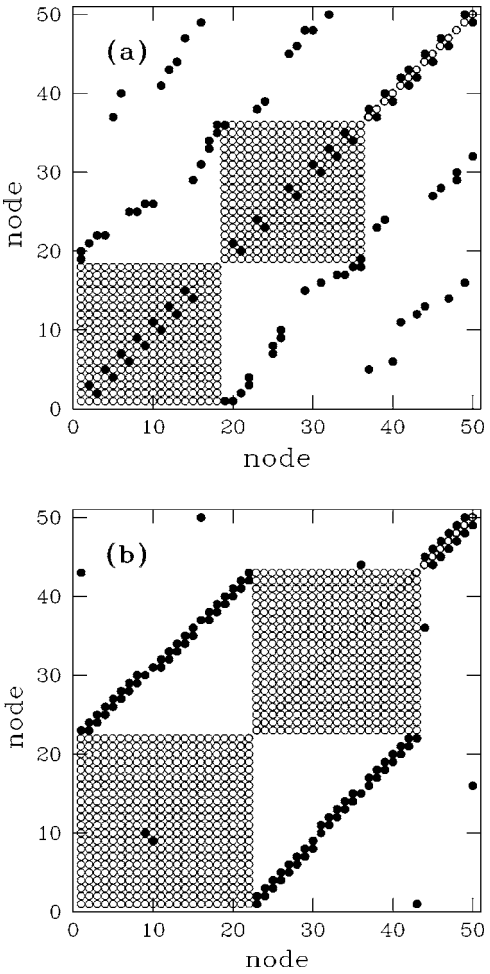

FIG. 13. The cluster formation for one-dimensional nearest neighbor network using node-node plot as in Fig. 3. (a) is for $g(x)=x$ and $\epsilon=0.30$ and (b) is for $g(x)=f(x)$ and $\epsilon=0.15$.

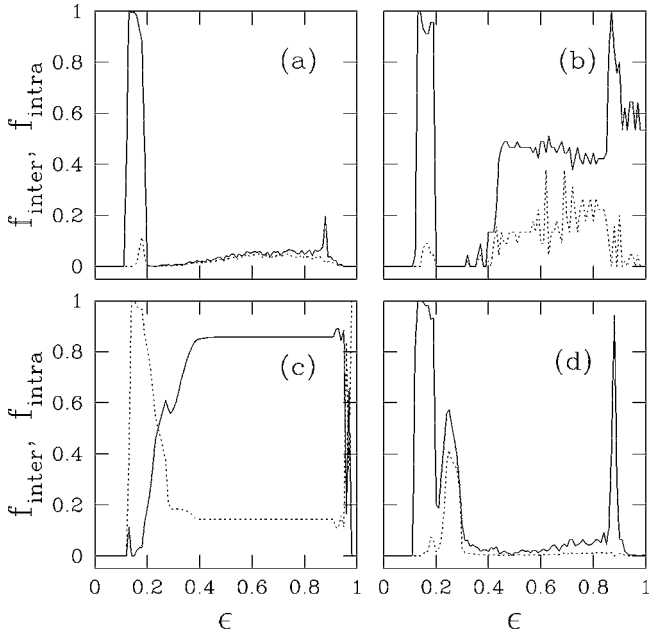

FIG. 15. (a) The fraction of intracluster and intercluster couplings, f_{inter} (solid line) and f_{intra} (dashed line), is shown as a function of the coupling strength ϵ for the small world network for $g(x)=f(x)$, respectively. Small world networks are generated for $N=50$, $m=1$, and $p=0.06$ [3]. (b) Same plot as in (a) but for the Caley tree with $g(x)=f(x)$ and $N=47$. Caley trees are generated with coordination number three [27]. (c) and (d) Same as in (a), but for two-dimensional lattice with $N=49$ and, respectively, for $g(x)=x$ and $g(x)=f(x)$.

C. Parameter variation

So far we have considered homogeneous coupled systems, i.e., with identical local dynamics. We now consider a situation of coupled systems where the maps are not identical but have some parameter mismatch. We have done some

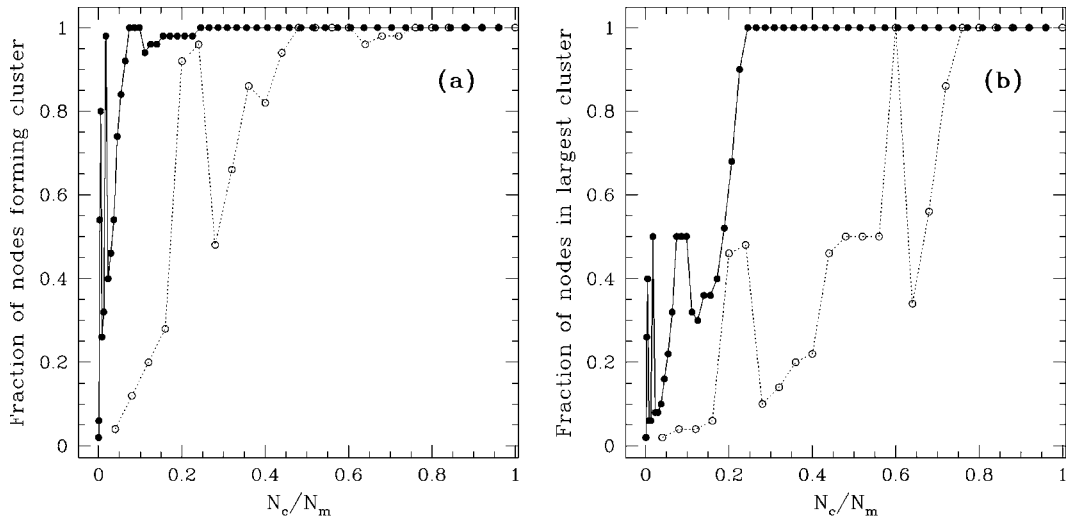

FIG. 14. (a) The fraction of nodes forming clusters as a function of the fraction of couplings N_c/N_m where $N_m=N(N-1)/2$. The figures are plotted for 1-dimensional coupled maps with $g(x)=f(x)$ and for $\epsilon=0.49$ (closed circles) and $\epsilon=0.7$ (open circles). The results are for $N=50$ and are obtained by averaging over 100 random initial conditions. (b) The fraction of nodes in the largest cluster as a function of N_c/N_m for $\epsilon=0.49$ (closed circles) and $\epsilon=0.7$ (open circles). Other parameters are the same as in (a).

preliminary calculations of synchronization in such systems. We vary the parameter μ of the logistic map first with a linear increase

$$\mu_i = 4.0 - \frac{i}{N}, \quad i = 1, \ldots, N$$

and secondly with a random distribution in a range $(4.0-\Delta\mu, 4.0)$. (For the linear change of μ in random and other similar networks the ordering of the node indices is arbitrary.)

For small coupling strength (region II) the driven behavior is somewhat strengthened while for large coupling strength there is not much variation. The region of complete synchronization shows a slight decrease.

How does the transition to complete synchronization take place? Opisov *et al.* [71] have analyzed coupled Rössler and coupled circle maps and found that there are two ways in which transition to complete synchronization takes place: soft and hard. In these studies, the state with no parameter mismatch is always the state of complete synchronization. The soft transition takes place without cluster formation and occurs when the parameter mismatch is smaller while the hard transition takes place through formation of smaller clusters and it occurs when the parameter mismatch is larger. The case of synchronization in complex networks that we are considering is somewhat different. We have cluster formation even when there is no parameter mismatch. However, it is interesting to see how the transitions occur in our case as the coupling strength is varied. Let us first consider the case of a small number of connections ($\sim N$). As the coupling strength increases we get synchronization around $\epsilon = 0.2$ (region II). This transition is soft, i.e., without clusters. However, the desynchronization for further increase in the coupling strength is a hard transition and several smaller clusters are formed. Again the transition to complete synchronization for large coupling strength is hard. Second, when the number of connections are increased ($\sim N^2$) the self-organized state is favored and in this case the transition to a completely synchronized state is hard.

D. Example

There are several examples of self-organized and driven behavior in naturally occurring systems. An important example in physics that includes both self-organized and driven behavior is the nearest neighbor Ising model treated using Kawasaki dynamics. As the strength of Ising interaction between spins changes sign from positive to negative there is a change of phase from a ferromagnetic (self-organized) to an antiferromagnetic (driven) behavior. In the ferromagnetic phase, domains (or clusters) of spins aligned in the same direction can be observed. In the antiferromagnetic state, i.e., driven behavior, the lattice spits into two sublattices with opposite spin states and having only intercluster interactions and no intracluster interactions. Several other examples are discussed in Ref. [55]. Several natural systems show examples of floating nodes, e.g., some birds may show intermittent behavior between free flying and flying in a flock.

V. CIRCLE MAP

We have studied the cluster formation with the circle map defining the local dynamics, given by

$$f(x) = x + \omega + (k/2\pi)\sin(2\pi x) \pmod 1. \tag{7}$$

Due to the modulo condition, instead of using the variable x_t, we use a function satisfying periodic boundary conditions, e.g., $\sin(\pi x_t)$, to decide the location of maxima and minima which are used to determine the phase synchronization of two nodes [Eq. (4)]. Here we discuss the results with the parameters of the circle map in the chaotic region ($\omega = 0.44$ and $k = 6$). For linear coupling $g(x) = x$ and scale-free networks with $m = 1$, for small coupling strength nodes evolve chaotically with no cluster formation (turbulent region). As the coupling strength increases nodes form clusters for $0.21 < \epsilon < 0.25$. In most of this region the nodes form two dominant driven clusters, except in the initial part, $\epsilon \approx 0.21$, where self-organized clusters can be observed. As the coupling strength increases nodes behave in a turbulent manner and after $\epsilon > 0.60$ nodes form clusters of dominant driven type. Here the number of nodes forming clusters and the sizes of clusters, both are small. For the one-dimensional linearly coupled network with $m = 1$, for linear coupling the nodes form phase synchronized clusters for the coupling strength region $0.21 < \epsilon < 0.25$. The clusters are mainly of the driven type except in the initial part, $\epsilon \approx 0.21$, where they are of the self-organized type. For large coupling strength they do not show any cluster formation.

For $g(x) = f(x)$ we found very negligible cluster formation for the entire range of the coupling strength for both scale-free and one-dimensional network with $m = 1$. However, as m increases the nodes form phase synchronized clusters for ϵ larger than some critical ϵ_c.

For the circle map the normalization factor $(1-\epsilon)$ in the first term of Eq. (1) is not necessary and the following modified model can also be considered.

$$x_{t+1}^i = f(x_t^i) + \frac{\epsilon}{k_i} \sum_{j=1}^{N} C_{ij} g(x_t^j) \pmod 1. \tag{8}$$

We now discuss the synchronized cluster formation for the same parameter values as above ($\omega = 0.44$ and $k = 6$) for this modified model. For linear coupling $[g(x) = x]$, clusters are formed only for $0.02 < \epsilon < 0.17$ with dominant self-organized behavior for most of the range except near $\epsilon \approx 0.17$ where the behavior is of dominant driven type. For the scale-free networks ($m = 1$) we have ordered states while for the one-dimensional networks we have partially ordered states. For nonlinear coupling $[g(x) = f(x)]$, the clusters are formed for $0.0 < \epsilon < 0.09$. The scale-free networks show mostly mixed clusters while one-dimensional networks show dominant self-organized clusters. There is no cluster formation for larger coupling strengths for both linear and nonlinear coupling. However, as for the logistic map, synchronized clusters are observed for large ϵ as the number of connections increases.

VI. CONCLUSION AND DISCUSSION

We have studied the properties of coupled dynamical elements on different types of networks. We find that in the course of time evolution they form phase synchronized clusters. We have mainly studied networks with a small number of connections ($N_c \sim N$) because a large number of natural systems fall under this category of a small number of connections. More importantly, with a small number of connections, it is easy to identify the relation between the dynamical evolution, the cluster formation, and the geometry of networks. We have studied the behavior of individual nodes, either forming clusters or evolving independently, and also the mechanism of cluster formation.

In several cases when synchronized clusters are formed there are some isolated nodes which do not belong to any cluster. More interestingly there are some *floating* nodes which show an intermittent behavior between an independent evolution and an evolution synchronized with some cluster. The residence time spent by a floating node in the synchronized cluster shows an exponential distribution.

We have identified two mechanisms of cluster formation, self-organized and driven phase synchronization. By considering the number of inter- and intra-cluster couplings we can identify phase synchronized clusters with dominant self-organized behavior (S), dominant driven behavior (D), and mixed behavior (M) where both mechanisms contribute. We have also observed ideal clusters of both self-organized and driven type. In most cases where ideal behavior is observed, the largest Lyapunov exponent is negative or zero giving stable clusters with periodic evolution. However, in some cases ideal behavior is also observed in the chaotic region.

By defining different states of the dynamical system using the number and type of clusters, we consider the phase-diagram in the $\mu-\epsilon$ plane for the local dynamics governed by the logistic map. When the local dynamics is in the chaotic region, for small coupling strengths we observe turbulent behavior. There is a critical value ϵ_c above which phase synchronized clusters are observed. The critical value depends on the type of network and the coupling function. For $g(x)=x$ type of coupling, self-organized clusters are formed when the strength of the coupling is small. As the coupling strength increases there is a crossover from the self-organized to the driven behavior which also involves reorganization of nodes into different clusters. This behavior is almost independent of the type of network. For the nonlinear diffusive coupling of type $g(x)=f(x)$, for small coupling strength phase synchronized clusters of driven type are formed, but for large coupling strength the number of nodes forming clusters as well as sizes of clusters both are very small and almost negligible for many networks. Only scale-free networks and Caley tree show some cluster formation for large coupling strengths.

As the number of connections increases, most of the clusters become of the mixed type where both the mechanisms contribute. We find that in general, the self-organized behavior is strengthened and also the number of nodes forming clusters as well as the size of clusters increase. As the number of connections become of the order of N^2, self-organized behavior with a single spanning cluster is observed for ϵ larger than some value.

It is interesting to consider the dynamical origin of the self-organized and driven phase synchronization and of floating nodes. A clue can be obtained by considering some tailor-made networks such as globally coupled networks and complete bipartite networks. These are considered in Part II [72].

ACKNOWLEDGMENTS

This work was partly supported by National Science Council of Taiwan under Grant No. NSC 92-2112-M 001-063 and Academia Sinica under Grant No. AS-91-TP-A02. One of us (R.E.A.) would like to thank Physics Division of National Center for Theoretical Sciences at Taipei and Institute of Physics of Academia Sinica for hospitality where the final version of this paper was done.

APPENDIX

Here we show that the definition (4) of phase distance d_{ij} between two nodes i and j satisfies metric properties. Let $\mathcal{N}_i$ denote the set of minima of the variable x_t^i in a time interval T. The phase distance satisfies the following metric properties.

(A) $d_{ij}=d_{ji}$.

(B) $d_{ij} \geqslant 0$ and the equality hold only if $\mathcal{N}_i=\mathcal{N}_j$.

(C) Triangle inequality: Consider three nodes i, j, and k. Denoting the number of elements of a set by $|.|$, let

(1) $a=|\mathcal{N}_i \cap \mathcal{N}_j \cap \mathcal{N}_k|$.

(2) $b=|\mathcal{N}_i \cap \mathcal{N}_k|-a$.

(3) $c=|\mathcal{N}_j \cap \mathcal{N}_k|-a$.

(4) $d=|\mathcal{N}_i \cap \mathcal{N}_j|-a$.

(5) $e=|\mathcal{N}_i|-b-d-a$.

(6) $f=|\mathcal{N}_j|-c-d-a$.

(7) $g=|\mathcal{N}_k|-b-c-a$.

We have

$$n_{ik}=a+b,$$

$$n_{jk}=a+c,$$

$$n_{ij}=a+d,$$

$$n_i=a+b+d+e,$$

$$n_j=a+c+d+f,$$

$$n_k=a+b+c+g.$$

Consider the combination

$$d_{ik}+d_{jk}-d_{ij}=1-X \tag{A1}$$

where

$$X=\frac{n_{ik}}{\max(n_i,n_k)}+\frac{n_{jk}}{\max(n_j,n_k)}-\frac{n_{ij}}{\max(n_i,n_j)}.$$

The triangle inequality is proved if $X \leqslant 1$. Consider the following three general cases.

Case a. $n_i \leqslant n_j \leqslant n_k$:

$$X = \frac{a+b}{n_k} + \frac{a+c}{n_k} - \frac{a+d}{n_j} \leqslant \frac{a+b+c-d}{n_k} \leqslant 1. \quad \text{(A2)}$$

Case b. $n_i \leqslant n_k \leqslant n_j$:

$$X = \frac{a+b}{n_k} + \frac{a+c}{n_j} - \frac{a+d}{n_j} \leqslant \frac{a+b+c}{n_k} \leqslant 1. \quad \text{(A3)}$$

Case c. $n_k \leqslant n_i \leqslant n_j$:

$$X = \frac{a+b}{n_i} + \frac{a+c}{n_j} - \frac{a+d}{n_j} \leqslant \frac{a+b+c}{n_i} \leqslant \frac{a+b+c}{n_k} \leqslant 1. \quad \text{(A4)}$$

This proves the triangle inequality.

[1] S. H. Strogatz, Nature (London) **410**, 268 (2001), and references therein.
[2] R. Albert and A. L. Barabäsi, Rev. Mod. Phys. **74**, 47 (2002), and references therein.
[3] D. J. Watts and S. H. Strogatz, Nature (London) **393**, 440 (1998).
[4] A.-L. Barabäsi and R. Albert, Science **286**, 509 (1999).
[5] C. Koch and G. Laurent, Science **284**, 96 (1999).
[6] S. Wasserman and K. Faust, *Social Network Analysis* (Cambridge University Press, Cambridge, England, 1994).
[7] R. Albert, H. Jeong, and A.-L. Barabäsi, Nature (London) **401**, 130 (1999); **406**, 378 (2000).
[8] H. Jeong, B. Tomber, R. Albert, Z. N. Oltvai, and A.-L. Barabäsi, Nature (London) **407**, 651 (2000).
[9] Richard J. Williams and Nea D. Martinez, Nature (London) **404**, 180 (2000).
[10] S. Render, Eur. Phys. J. B **4**, 131 (1998); M. E. J. Newman, Phys. Rev. E **64**, 016131 (2001).
[11] K. Kaneko, Prog. Theor. Phys. **72**, 480 (1984).
[12] K. Kaneko, Physica D **34**, 1 (1989), and references therein.
[13] K. Kaneko, Phys. Rev. Lett. **65**, 1391 (1990); Physica D **41**, 137 (1990); **124**, 322 (1998).
[14] D. H. Zanette and A. S. Mikhailov, Phys. Rev. E **57**, 276 (1998).
[15] N. J. Balmforth, A. Jacobson, and A. Provenzale, Chaos **9**, 738 (1999).
[16] O. Popovych, Y. Maistenko, and E. Mosekilde, Phys. Lett. A **302**, 171 (2002).
[17] G. I. Menon, S. Sinha, and P. Ray, e-print cond-mat/0208243.
[18] O. Popovych, A. Pikovsky, and Y. Maistrenko, Physica D **168–169**, 106 (2002).
[19] G. Abramson and D. H. Zanette, Phys. Rev. E **58**, 4454 (1998).
[20] A. Lemaître and H. Chate, Phys. Rev. Lett. **82**, 1140 (1999).
[21] N. B. Ouchi and K. Kaneko, Chaos **10**, 359 (2000).
[22] H. Chate and P. Manneville, Europhys. Lett. **17**, 291 (1992); Chaos **3**, 307 (1992).
[23] P. M. Gade, Phys. Rev. E **54**, 64 (1996).
[24] S. C. Manrubia and A. S. Mikhailov, Phys. Rev. E **60**, 1579 (1999).
[25] Y. Zhang, G. Hu, H. A. Cerderia, S. Chen, T. Barun, and Y. Yao, Phys. Rev. E **63**, 026211 (2001).
[26] S. Sinha, Phys. Rev. E **66**, 016209 (2002).
[27] P. M. Gade, H. A. Cerderia, and R. Ramaswamy, Phys. Rev. E **52**, 2478 (1995).
[28] P. M. Gade and C.-K. Hu, Phys. Rev. E **62**, 6409 (2000).
[29] H. Hong, M. Y. Choi, and B. J. Kim, Phys. Rev. E **65**, 026139 (2002); **65**, 047104 (2002).
[30] T. Nishikawa, A. E. Motter, Y. C. Lai, and F. C. Hoppensteadt, Phys. Rev. Lett. **91**, 014101 (2003).
[31] N. J. Balmforth, A. Provenzale, and R. Sassi, Chaos **12**, 719 (2002).
[32] S. E. de S. Pinto and R. L. Viana, Phys. Rev. E **61**, 5154 (2000).
[33] H. Fujisaka and T. Yamada, Prog. Theor. Phys. **69**, 32 (1983).
[34] M. Ding and W. Yang, Phys. Rev. E **56**, 4009 (1997).
[35] M. Soins and S. Zhou, Physica D **165**, 12 (2002).
[36] J. Jost and M. P. Joy, Phys. Rev. E **65**, 016201 (2002).
[37] Y. L. Maistrenko, V. L. Maistrenko, O. Popovych, and E. Mosekilde, Phys. Rev. E **60**, 2817 (1999).
[38] R. E. Amritkar, P. M. Gade, A. D. Gangal, and V. M. Nandkumaran, Phys. Rev. A **44**, R3407 (1991).
[39] R. E. Amritkar, Physica A **224**, 382 (1996).
[40] E. Olbrich, R. Hegger, and H. Kantz, Phys. Rev. Lett. **84**, 2132 (2000).
[41] P. Garcïa, A. Parravano, M. G. Cosenza, J. Jimënez, and A. Marcano, Phys. Rev. E **65**, 045201 (2002).
[42] L. Cisneros, J. Jimënez, M. G. Cosenza, and A. Parravano, Phys. Rev. E **65**, 045204 (2002).
[43] H. Aref, Annu. Rev. Fluid Mech. **15**, 345 (1983).
[44] A. Hilgers *et al.*, Europhys. Lett. **45**, 552 (1999).
[45] G. Perez, C. Pando-Lambruschini, S. Sinha, and H. A. Cerderia, Phys. Rev. A **45**, 5469 (1992).
[46] E. A. Jackson and A. Kodogeorgiou, Phys. Lett. A **168**, 270 (1992).
[47] T. Yanagita and K. Kaneko, Phys. Lett. A **175**, 415 (1993).
[48] C. Tsallis, A. M. C. de Souza, and E. M. F. Curado, Chaos, Solitons Fractals **6**, 561 (1995); W. J. Ma, C.-K. Hu, and R. E. Amritkar, Phys. Rev. E **70**, 026101 (2004).
[49] R. J. Hendry, J. M. McGlade, and J. Weiner, Ecol. Modell. **84**, 81 (1996).
[50] S. Sinha and W. L. Ditto, Phys. Rev. Lett. **81**, 2156 (1998).
[51] K. Aoki and N. Mugibayashi, Phys. Lett. A **128**, 349 (1998).
[52] F. A. Bignone, Theor. Comput. Sci. **217**, 157 (1999).
[53] C. Beck, Phys. Rev. D **69**, 123515 (2004).
[54] C. Beck, *Spatio-Temporal Chaos and Vacumum Fluctuations of Quantized Fields* (World Scientific, Singapore, 2002).
[55] S. Jalan and R. E. Amritkar, Phys. Rev. Lett. **90**, 014101 (2003).
[56] A. Pikovsky, M. Rosenblum, and J. Kurth, *Synchronization: A Universal Concept in Nonlinear Dynamics* (Cambridge University Press, Cambridge, England, 2001).
[57] S. Boccaletti, J. Kurth, G. Osipov, D. L. Valladares, and C. S. Zhou, Phys. Rep. **366**, 1 (2002).

[58] Y. Zhang, G. Hu, H. A. Cerdeira, S. Chen, T. Braun, and Y. Yao, Phys. Rev. E **63**, 026211 (2001).
[59] M. G. Rosenblum, A. S. Pikovsky, and J. Kurth, Phys. Rev. Lett. **76**, 1804 (1996); W. Wang, Z. Liu, and Bambi Hu, *ibid.* **84**, 2610 (2000).
[60] S. C. Manrubia and A. S. Mikhailov, Europhys. Lett. **53**, 451 (2001).
[61] N. B. Janson, A. G. Balanov, V. S. Anishchenko, and P. V. E. McClintock, Phys. Rev. Lett. **86**, 1749 (2001).
[62] H. L. Yang, Phys. Rev. E **64**, 026206 (2001).
[63] F. S. de San Roman, S. Boccaletti, D. Maza, and H. Mancini, Phys. Rev. Lett. **81**, 3639 (1998).
[64] In an earlier paper [55] we used the definition of phase distance as $d_{ij}=1-2\nu_{ij}/(\nu_i+\nu_j)$. However, this earlier definition does not satisfy the triangle inequality, while the definition given in this paper satisfies the same.
[65] S. C. Manrubia and A. S. Mikhailov, e-print cond-mat/9912054.
[66] A.-L. Barabasi, R. Albert, and H. Jeong, Physica A **281**, 69 (2000).
[67] As noted in Sec. III B, the self-organized splitting of a network into clusters is not unique. This can be seen by comparing Fig. 3(b) of this paper (two ideal self-organized clusters of sizes 41 and 9) and Fig. 1(a) of Ref. [55] (two ideal self-organized clusters of sizes 36 and 14) which are plotted for the same scale-free network and $g(x)=x$ but for different ϵ values. On the other hand the driven splitting is unique. This can be seen by comparing Fig. 3(d) of this paper and Fig. 1(b) of Ref. [55] which are again plotted for the same scale-free network but for different ϵ values.
[68] See, e.g., pp. 29, 54ff, and 107 of Ref. [54].
[69] S. Sinha, D. Biswas, M. Azam, and S. V. Lawande, Phys. Rev. A **46**, 6242 (1992).
[70] V. Ahlers and A. Pikovsky, Phys. Rev. Lett. **88**, 254101 (2002).
[71] G. V. Osipov, A. S. Pikovsky, M. G. Rosenblum, and J. Kurths, Phys. Rev. E **55**, 2353 (1997); G. V. Osipov and J. Kurths, *ibid.* **65**, 016216 (2001).
[72] R. E. Amritkar, S. Jalan, and C. K. Hu, Phys. Rev. E **72**, 016212 (2005).